Orientation of Amide-Nitrogen-15 Chemical Shift Tensors in Peptides: A Quantum Chemical Study

Jeffrey R. Brender,[†] Deanne M. Taylor,[†] and A. Ramamoorthy*[,†,‡,§]

Contribution from the Biophysics Research Division, Department of Chemistry, Macromolecular Science and Engineering, The University of Michigan, Ann Arbor, Michigan 48109-1055

Received June 5, 2000. Revised Manuscript Received October 27, 2000

Abstract: Knowledge of the orientation of the nitrogen-15 chemical shift anisotropy (CSA) tensor is critical for a variety of experiments that provide information on protein structure and dynamics in the solid and solution states. Unfortunately, the methods available for determining the orientation of the CSA tensor experimentally have inherent limitations. Rotation studies of a single crystal provide complete information but are tedious and limited in applicability. Solid-state NMR studies on powder samples can be applied to a greater range of samples but suffer from ambiguities in the results obtained. Density functional gauge-including-atomic-orbitals (GIAO) calculations of the orientations of ^{15}N CSA tensors in peptides are presented here as an independent source of confirmation for these studies. A comparison of the calculated ^{15}N CSA orientations with the available experimental values from single-crystal and powder studies shows excellent agreement after a partial, constrained optimization of some of the crystal structures used in the calculation. The results from this study suggest that the orientation as well as the magnitudes of ^{15}N CSA tensors may vary from molecule to molecule. The calculated α_N angle varies from 0° to 24° with the majority in the 10° to 20° range and the β_N angle varies from 17° to 24° in good agreement with most of the solid-state NMR experimental results. Hydrogen bonding is shown to have negligible effect on the orientation of ^{15}N CSA tensor in accordance with recent theoretical predictions. Furthermore, it is demonstrated that the orientation of the ^{15}N CSA can be calculated accurately with much smaller basis sets than is needed to calculate the chemical shift, suggesting that the routine application of ab initio calculations to the determination of ^{15}N CSA tensor orientations in large biomolecules might be possible.

Introduction

The study of chemical shift anisotropy (CSA) tensors in peptides and proteins has aroused considerable interest in recent years. The principal values and orientations of CSA tensors associated with the nuclei situated in the peptide plane provide a wealth of information that can be interpreted in terms of protein structure and dynamics in solid- as well as solution states. Several types of NMR studies on proteins are critically dependent on an accurate knowledge of CSA tensors: (1) the interpretation of the NMR spectra of uniaxially oriented systems such as peptides and proteins embedded in lipid bilayers,[1] (2) characterization of rapid, large-amplitude motions in solids,[2] (3) interpretation of the relaxation rates measured using solution NMR methods in terms of protein dynamics.[3] One of the most important CSA tensors for these studies is that of amide ^{15}N as it provides information on the primary and secondary structure of the peptide, electrostatics (including hydrogen bonding), solvation, and dynamics.[4−6] However, it is surprising that there are only very few well-characterized CSA tensors of amide ^{15}N reported so far in the literature. In fact, the only available single crystal study on the CSA tensor of amide ^{15}N could not yield the orientations of the principal axes, σ_{11N} and σ_{22N}, in the molecular frame because the tensor is very close to being axially symmetric.[7] Therefore, the orientations of the σ_{11N} and σ_{22N} axes (defined as $\sigma_{33N} \geq \sigma_{22N} \geq \sigma_{11N}$) are assumed only based on symmetry arguments. Often NMR studies on proteins assume ^{15}N CSA tensors with a fixed value and utilize the tensors that were determined from a model peptide. However, recent experimental measurements and theoretical ab initio predictions of amide ^{15}N CSA tensors have shown that the CSA tensor may vary substantially from compound to compound.[4,6,8,9] More CSA tensors therefore have to be well characterized to obtain accurate

* To whom correspondence should be addressed. Correspondence: A. Ramamoorthy; Telephone: (734)647-6572. Fax: (743)764-8776. E.mail: ramamoor@umich.edu.

† Biophysics Research Division.

‡ Department of Chemistry.

§ Macromolecular Science & Engineering.

(1) Fu, R. Q.; Cross, T. A. *Annu. Rev. Biophy. Biomol.* **1999**, *28*, 235−268. Ramamoorthy, A.; Marassi, F. M.; Zasloff, M.; Opella, S. J. *J. Biomol. NMR* **1995**, *6*, 329−334. Opella, S. J.; Marassi, F. M.; Gesell, J. J.; Valente, A. P.; Kim, Y.; Oblatt-Montal, M.; Montal, M. *Nat. Struct. Biol.* **1999**, *6*, 374−379.

(2) Scheurer, C.; Skrynnikov, N. R.; Lienin, S. F.; Straus, S. K.; Bruschweiler, R.; Ernst, R. R. *J. Am. Chem. Soc.* **1999**, *121*, 4242−4251.

(3) Tjandra, N.; Szabo, A.; Bax, A. *J. Am. Chem. Soc.* **1996**, *118*, 6986−6991. Palmer, A. G. *Curr. Opin. Struct. Biol.* **1997**, *7*, 732−737. Fischer, M. W. F.; Majumdar, A.; Zuiderweg, E. R. P. *Prog. Nucl. Magn. Reson. Spectrosc.* **1998**, *33*, 207−272. Fushman, D.; Tjandra, T.; Cowburn, D. *J. Am. Chem. Soc.* **1998**, *121*, 8577−8582. Kay, L. E. *Nat. Struct. Biol.* **1998**, *5*, 513−517.

(4) Lee, D. K.; Wittebort, R. J.; Ramamoorthy, A. *J. Am. Chem. Soc.* **1998**, *120*, 8868−8874.

(5) de Dios, A. C.; Pearson, J. G.; Oldfield, E. *Science* **1993**, 1491−1496.

(6) Lee, D. K.; Santos, J. S.; Ramamoorthy, A. *J. Phys. Chem. B* **1999**, *103*, 8383−8390. Lee, D. K.; Santos, J. S.; Ramamoorthy, A. *Chem. Phys. Lett.* **1999**, *309*, 209−214. Lee, D. K.; Wei, Y.; Ramamoorthy, A. *Chem. Phys. Lett.* In press. Lee, D. K.; Ramamoorthy, A. *J. Magn. Reson.* **1998**, *133*, 204−206. Wu, C. H.; Ramamoorthy, A.; Gierasch, L. M.; Opella, S. J. *J. Am. Chem. Soc.* **1995**, *117*, 6148−6149. Hong, M.; Gross, J. D.; Hu, W.; Griffin, R. G. *J. Magn. Reson.* **1998**, *135*, 169−177.

(7) Harbison, G. S.; Jelinski, L. W.; Stark, R. E.; Torchia, D. A.; Herzfeld, J.; Griffin, R. G. *J. Magn. Reson.* **1984**, *60*, 79−82.

10.1021/ja001980q CCC: $20.00
Published on Web 01/11/2001

results from structural studies on peptides and proteins using NMR spectroscopy.

While it is a simple matter to measure the magnitudes of the three principal elements of a CSA tensor directly from the discontinuities observed in a powder pattern, this typically provides no information about the orientation of the CSA tensor in the molecular frame. Traditionally, the only sure way to determine both magnitudes and orientations of the principal elements of a CSA tensor has been to perform a rotation study of a single crystal of a molecule whose structure has been determined by X-ray diffraction. However, these measurements can be tedious, and because they require large, high-quality single crystals, which can be difficult or impossible to obtain for many of the most interesting molecules, they are inherently limited to selected examples. Solid-state NMR experiments that correlate chemical shift and dipolar coupling parameters in one, two, or three dimensions have been used to characterize a number of different tensors in powder samples.[4,6,9] However, these studies cannot provide the unambiguous orientation of the CSA tensor in the molecular frame and thus depend on the results from a single-crystal study.

Quantum chemical calculations provide an independent source of confirmation on the orientation of the shielding tensor. Recent progress in quantum chemical methods for the calculation of CSA tensors allows applications to biological molecules of moderate size with increasingly quantitative agreement with experimental data. While several theoretical studies have reported CSA tensors and their dependence on backbone conformation, amino acid residue type, and hydrogen bonding in polypeptides and proteins, the focus of these studies has been primarily on the calculation of isotropic shifts and primarily on ^{13}C CSA tensors, where a simple correspondence between secondary structure and the isotropic chemical shift was observed.[2,8,10−18] Although an ab initio study of the orientation of the ^{15}N CSA tensors in proteins has been performed before to qualitatively study the influence of secondary structure and hydrogen bonding on the CSA tensor,[8] a direct quantitative comparison of ab initio to experimental CSA tensors in peptides has been, with very few exceptions, lacking.[2,15,18] Quantitative accuracy in the orientation of the CSA tensor is important for the applications to structural questions in solid-state NMR that depend on subtle differences in CSA orientation.[1,2,9,19−22] We therefore thought it is worthwhile to investigate the use of ab initio calculations to quantitatively determine the ^{15}N CSA tensor orientations in peptides using experimental geometries.

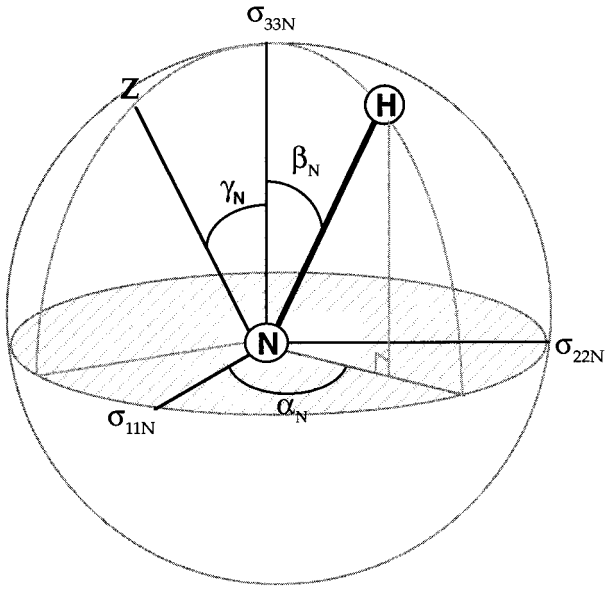

Figure 1. Orientations of the principal axes of the ^{15}N chemical shift tensor relative to the N−H bond and the peptide plane. γ_N is the angle between σ_{33N} and the projection of σ_{33N} onto the peptide plane (represented by the vector Z). β_N is the angle between the σ_{33N} axis and the N−H bond. α_N is the angle between σ_{11N} and the projection of the N−H bond on the σ_{11N} $-\sigma_{22N}$ plane.

Methods

The complete description of a CSA tensor requires the magnitudes of its principal elements and three Euler angles (α_N, β_N, γ_N) describing the orientation of the principal axis system (PAS) in the molecular frame (see Figure 1). The angle α_N is defined as the angle between σ_{11N} and the projection of the N−H bond onto the $\sigma_{11N}-\sigma_{22N}$ plane. The angle β_N is defined as the angle between σ_{33N} and the N−H bond, and the angle γ_N is defined as the angle between the peptide plane and the σ_{33N} axis. The α_N and β_N angles are sufficient to completely describe the orientation of the PAS about the N−H bond and are accessible from solid-state NMR studies on powdered samples.[4] Relating the orientation of PAS to the peptide plane and not just to the N−H bond

(8) Walling, A. E.; Pargas, R. E.; de Dios, A. C. *J. Phys. Chem. A* **1997**, *101*, 7299−7303.

(9) Mai, W.; Hu, W.; Wang, C.; Cross, T. A. *Protein Sci.* **1993**, *2*, 532−542.

(10) Ando, I.; Saito, H.; Tabeta, R.; Shoji, A.; Ozaki, T. *Macromolecules* **1984**, *17*, 457−461. Ando, S.; Ando, I.; Shoji, A.; Ozaki, T. *J. Am. Chem. Soc.* **1988**, *110*, 3380−3386. Chestnut, D. B. *Rev. Comput. Chem.* **1996**, *8*, 245−295. Chestnut, D. B.; Phung, C. G. *Chem. Phys. Lett.* **1993**, *183*, 505−509. de Dios, A. C.; Laws, D. D.; Oldfield, E. *J. Am. Chem. Soc.* **1994**, *116*, 7784−7786.

(11) Havlin, R. H.; Le, H.; Laws, D. D.; de Dios, A. C.; Oldfield, E. *J. Am. Chem. Soc.* **1997**, *119*, 11951−11958. Heller, J.; Laws, D. D.; Tomaselli, M.; King, D. S.; Wemmer, D. E.; Pines, A.; Havlin, R. H.; Oldfield, E. *J. Am. Chem. Soc.* **1997**, *119*, 7827−7831. Le, H.; Pearson, J. G.; de Dios, A. C.; Oldfield, E. *J. Am. Chem. Soc.* **1995**, *117*, 3800−3807. Sitkoff, D.; Case, D. A. *Prog. Nucl. Magn. Reson. Spectrosc.* **1998**, 165−190. Ludwig, R.; Weinhold, F.; Farrar, T. C. *J. Phys. Chem. A* **1997**, *101*, 8861−8870. Pearson, J. G.; Le, H.; Sanders, L. K.; Godbout, N.; Havlin, R. H.; Oldfield, E. *J. Am. Chem. Soc.* **1997**, *119*, 11941−11950. Pearson, J. G.; Wang, J. F.; Markley, J. L.; Le, H.; Oldfield, E. *J. Am. Chem. Soc.* **1995**, *117*, 8823−8829. Sulzbach, H. M.; Schleyer, P.; Schaefer, H. F. *J. Am. Chem. Soc.* **1995**, *117*, 2632−2637. Wei, Y. F.; de Dios, A. C.; McDermott, A. E. *J. Am. Chem. Soc.* **1999**, *121*, 10389−10394. De Dios, A. C. *Prog. Nucl. Magn. Reson. Spectrosc.* **1996**, *29*, 229−278. Fukui, H. *Prog. Nucl. Magn. Reson. Spectrosc.* **1997**, *31*, 317−342. De Dios, A. C. *Solid State NMR Spectrosc.* **1996**, *6*, 101−125. Sulzbach, H. M.; Vacek, G.; Schreiner, P. R.; Galbraith, J. M.; Schleyer, P. V. R.; Schaefer, H. F. *J. Comput. Chem.* **1997**, *18*, 126−138. Perczel, A.; Császár, A. G. *J. Comput. Chem.* **2000**, *21*, 882−900. Pecul, M.; Leszczynski, J.; Sadlej, J. *J. Phys. Chem. A* **2000**, *104*, 8105−8111.

(12) Herzfeld, J.; Olbris, D. J.; Furman, E.; Benderskiy, V. *J. Chem. Phys.* **2000**, *113*, 5162−5170.

(13) Woolf, T. B.; Malkin, V. G.; Malkina, O. L.; Salahub, D. R.; Roux, B. *Chem. Phys. Lett.* **1995**, *239*, 186−194.

(14) Kowalewski, J.; Werbelow, L. *J. Magn. Reson.* **1997**, *128*, 144−148.

(15) Ferraro, M. B.; Repetto, V.; Facelli, J. C. *Solid State Nucl. Magn. Reson.* **1998**, *10*, 185−189.

(16) Malkin, V. G.; Malkina, O. L.; Salahub, D. R. *J. Am. Chem. Soc.* **1995**, *117*, 3294−3295.

(17) Le, H. B.; Oldfield, E. *J. Phys. Chem.* **1996**, *100*, 16423−16428.

(18) Facelli, J. C.; Pugmire, R. J.; Grant, D. M. *J. Am. Chem. Soc.* **1996**, *118*, 5488−5489.

(19) Hong, M.; Gross, J. D.; Griffin, R. G. *J. Phys. Chem B.* **1997**, *101*, 5869−5874. Smith, S. O. *Q. Rev. Biophys.* **1996**, *29*, 395−449.

(20) Nicholson, L. K.; Teng, Q.; Cross, T. A. *J. Mol. Biol.* **1991**, *218*, 621−637. Ketchem, R. R.; Lee, K.-C.; Huo, S.; Cross, T. A. *J. Biomol. NMR* **1996**, *8*, 1−14.

(21) Ramamoorthy, A.; Marassi, F. M.; Opella, S. J. In *Proceedings of the International School of Biological Magnetic Resonance, 2nd Course, Dynamics and the Problem of Recognition in Biological Macromolecules*; Jardetsky, O., Lefeure, J., Eds.; Plenum: New York, 1996; Chapter 17, pp 237−255. Cross, T. A.; Opella, S. J. *Curr. Opin. Struct. Biol.* **1994**, *4*, 574−581.

(22) Fushman, D.; Cowburn, D. *J. Biomol. NMR* **1999**, *13*, 139−147. Kroenke, C. D.; Rance, M.; Palmer, A. G., III. *J. Am. Chem. Soc.* **1999**, *121*, 10119−10125.

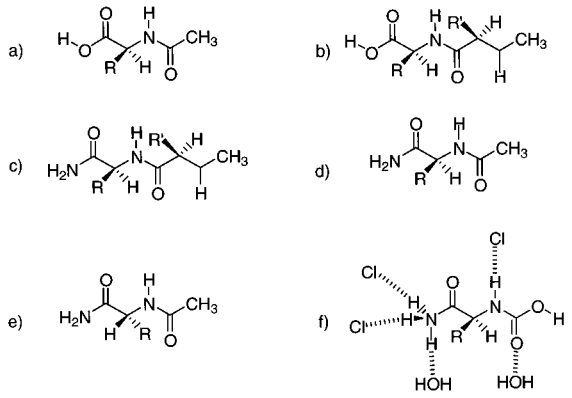

Figure 2. Structures of molecules used in the calculations. (a) *N*-acetyl compounds of type NAR where R is the side chain of E, G, C, M, A, or V amino acid residues. (b) *N*-acetyl-valyl-leucine (NAVL). (c) *N*-acetyl amide dipeptides of type NAR′RA where R′ = CH_3 and R = H, R′ = CH_3 and R = CH_3, R′ = indole ring and R = H. (d) *N*-acetyl amide compounds of type NARA where R is the side chain of valine or glycine. (e) D,L-NAA. (f) GG·HCl·H_2O

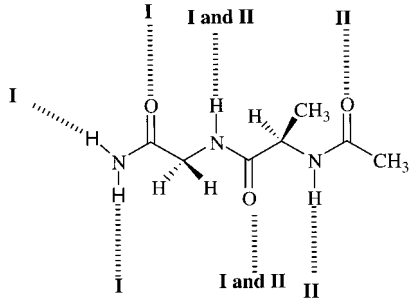

Figure 3. Illustration of the hydrogen bonding used for the calculation of ^{15}N CSA from *N*-acetyl-glycyl-glycine-amide (NAGAA) molecule. A total of three calculations were performed as follows. The first calculation was performed without hydrogen bonding, and then the second and third calculations were performed with hydrogen-bonding sets I and II, respectively, as shown. The difference from the full hydrogen-bonding pattern was estimated by comparing the calculated α_N and β_N values using set I against set II. The difference was found to be negligible (0.5° change in α_N and 0.2° change in β_N) compared to experimental errors.

requires the third Euler angle γ_N. This angle is not accessible from solid-state NMR studies on powdered samples and must be determined from a solid-state NMR study on a single crystal. The rotation matrix relating PAS to the molecular axis system can be written as:

$$R\begin{bmatrix}x\\y\\z\end{bmatrix}=\begin{bmatrix}-\sin(\gamma)\cos(\alpha)+\cos(\gamma)\cos(\beta)\cos(\alpha) & \sin(\gamma)\sin(\alpha)+\sin(\gamma)\cos(\beta)\cos(\alpha) & -\cos(\gamma)\sin(\beta)\\ -\sin(\gamma)\cos(\alpha)-\sin(\gamma)\cos(\beta)\sin(\alpha) & \cos(\gamma)\cos(\alpha)-\sin(\gamma)\cos(\beta)\cos(\alpha) & \sin(\gamma)\sin(\beta)\\ \sin(\beta)\cos(\alpha) & \sin(\beta)\cos(\alpha) & \cos(\beta)\end{bmatrix}\begin{bmatrix}x\\y\\z\end{bmatrix}$$

where *y* is in the direction of the N−H bond, *z* is perpendicular to the peptide plane, and *x* is perpendicular to each.

The molecules in this study were chosen to reflect a reasonable amount of diversity in primary and secondary structures and at the same time small enough in size to be computationally tractable. The molecular structures shown in Figure 2 were taken directly from the crystal structures listed without further refinement.[23−34] Two sets of ab initio calculations were carried out on most of the molecules studied in this work. The first set of calculations consisted of the molecules in isolation (that is without the hydrogen bonding), and the second set of calculations consisted of the molecule surrounded by its complete set of hydrogen bonding partners taken directly from the crystallographic coordinates. The calculations performed on *N*-acetyl-valyl-leucine (NAVL), D,L-*N*-acetyl-leucine amide (D,L-NALA), and *N*-acetyl-glycyl-alanine amide (NAGAA) are exceptions to this general procedure as explained below. (1) NAVL and D,L-NALA proved to be too large for this method to be tractable. The valine and leucine residues were therefore replaced, for the hydrogen bonding partners only, with alanine residues by the truncation of the side chain which was then energetically minimized by molecular mechanics using the MM2 force field. (2) The dipeptide NAGAA was also too large for the general method outlined above to be practical. The hydrogen bonding scheme outlined in Figure 3 was used instead.

The basis set used was a locally dense 6-311G (2d, p) basis set on the atoms shown in bold below:[35]

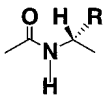

The local basis approximation has been previously shown to be excellent for chemical shift calculations.[36] The D95 basis set was applied to the remainder of the molecule and on the hydrogen bonding partners.[37] The gauge-independence requirement was treated with the gauge-including atomic orbitals (GIAO)[38] approach as implemented in Gaussian 98.[39] All calculations used the Perdew−Wang-91 (PW91) exchange-correlation potential.[40] This procedure generates a second rank asymmetric tensor which can then be decomposed into a scalar tensor of rank 1 and an antisymmetric tensor and a symmetric tensors of rank

(23) Carroll, P. J.; Stewart, P. L.; Opella, S. J. *Acta Crystallogr., Sect.C* **1990**, *46*, 243−246.
(24) Dobson, A.; Gerkin, R. *Acta Crystallogr., Sect. C* **1997**, 53.
(25) Donohue, J.; Marsh, R. *Acta Crystallogr.* **1962**, *15*, 941−945.
(26) Koetzle, T. F.; Hamilton, W. C.; Parthasarathy, R. *Acta Crystallogr., Sect. B* **1972**, *28*, 2083−2091.
(27) Puliti, R.; Mattia, C. A.; Barone, G.; Giancola, C. *Acta Crystallogr., Sect. C* **1991**, *47*, 581.
(28) Ponnuswamy, M. N.; Trotter, J. *Acta Crystallogr.* **1985**, *C41*, 917−919.
(29) Puliti, R.; Mattia, C. A.; Barone, G.; Giancola, C. *Acta Crystallogr., Sect. C* **1989**, *45*, 1554−1557.
(30) Puliti, R.; Mattia, C. A.; Barone, G.; Gatta, D. G.; Ferro, D. *Thermochim. Acta* **1990**, *162*, 229−240.
(31) Puliti, R.; Mattia, C. A.; Lilley, T. H. *Acta Crystallogr., Sect. C* **1993**, *49*, 2173−2179.
(32) Puliti, R.; Mattia, C. A. *Acta Crystallogr.* **1995**, *C51*, 336−339.
(33) Puliti, R.; Barone, G.; Giancola, C.; Mattia, C. A. *J. Mol. Struct.* **1996**, *382*, 197−203.
(34) Takusagawa, F.; Koetzle, T. F.; Kou, W. W. H.; Parthasarathy, R. *Acta Crystallogr., Sect. B* **1981**, *37*, 1591−1596.
(35) Dewar, M. J. S.; Reynolds, C. H. *J. Comput. Chem.* **1986**, *2*, 140−151.
(36) Chestnut, D. B.; Moore, K. D. *J. Comput. Chem.* **1989**, *10*, 648−659. Chestnut, D. B.; Rusiloski, B. E.; Moore, K. D.; Egolf, D. A. *J. Comput. Chem.* **1993**, *14*, 1364−1375.
(37) Dunning, T. H.; Hay, P. J. In *Modern Theoretical Chemistry*; Schaefer, H. F, Ed.; Plenum: New York, 1976; Vol. 3.
(38) Ditchfield, R. *Mol Phys.* **1974**, *27*, 789. Wolinski, K.; Hinton, J. F.; Pulay, P. *J. Am. Chem. Soc.* **1990**, *112*, 8251. Rauhut, G.; Puyear, S.; Wolinski, K.; Pulay, P. *J. Phys. Chem.* **1996**, *100*, 6310. London, F. *J. Phys. Radium* **1937**, *8*, 397.
(39) Frisch, M. J.; Trucks, G. W.; Schlegel, H. B.; Scuseria, G. E.; Robb, M. A.; Cheeseman, J. R.; Zakrzewski, V. G.; Montgomery, J. A., Jr.; Stratmann, R. E.; Burant, J. C.; Dapprich, S.; Millam, J. M.; Daniels, A. D.; Kudin, K. N.; Strain, M. C.; Farkas, O.; Tomasi, J.; Barone, V.; Cossi, M.; Cammi, R.; Mennucci, B.; Pomelli, C.; Adamo, C.; Clifford, S.; Ochterski, J.; Petersson, G. A.; Ayala, P. Y.; Cui, Q.; Morokuma, K.; Malick, D. K.; Rabuck, A. D.; Raghavachari, K.; Foresman, J. B.; Cioslowski, J.; Ortiz, J. V.; Stefanov, B. B.; Liu, G.; Liashenko, A.; Piskorz, P.; Komaromi, I.; Gomperts, R.; Martin, R. L.; Fox, D. J.; Keith, T.; Al-Laham, M. A.; Peng, C. Y.; Nanayakkara, A.; Gonzalez, C.; Challacombe, M.; Gill, P. M. W.; Johnson, B. G.; Chen, W.; Wong, M. W.; Andres, J. L.; Head-Gordon, M.; Replogle, E. S.; Pople, J. A. *Gaussian 98*, revision A; Gaussian, Inc.: Pittsburgh, PA, 1998.
(40) Perdew, J. P.; Wang, Y. *Phys. Rev. B* **1992**, *45*, 13244.

Table 1. Quantum Chemical Calculations of Amide-^{15}N Chemical Shift Tensors in Peptides

molecule		σ_{isoN}[a]	σ_{33N}	σ_{22N}	σ_{11N}	α_N[b]	β_N	γ_N	ref
D,L-*N*-acetyl-A-amide	(D,L-NAA)	106	218	88	10	17.1	14.4	3.2	27
with H bonds		116	232	80	36	12.6	16.2	0.1	
L- *N*-acetyl-A-amide	(L-NAA)	123	226	114	29	10.1	11.8	4.3	29
with H bonds		133	244	99	53	13.2	14.9	−5.6	
N-acetyl-*AA-amide	(NAAAA)	107	216	87	19	16.4	16.7	−3.8	32
with H bonds		118	233	81	41	15.5	17.1	3.1	
N-acetyl-A*A-amide	(NAAAA)	101	203	78	22	10.8	15.4	−3.1	32
with H bonds		115	222	72	50	20.7	16.5	4.3	
N-acetyl-G*A-amide	(NAGAA)	109	216	102	10	32.5	21.9	2.5	32
with H bonds		118	229	90	36	35.0	22.9	1.7	
N-acetyl-*GA-amide	(NAGAA)	105	208	90	19	3.5	15.1	−3.3	32
with H bonds		117	225	81	44	1.0	18.0	−2.6	
experimental		120	229	85	45	−	20.5 ± 2	−	42
N-acetyl-M	(NAM)	96	207	79	0	18.6	17.2	−6.1	28
with H bonds		103	214	77	17	16.8	18.1	−6.5	
N-acetyl-C	(NAC)	115	214	107	24	3.0	17.6	0.1	34
with H bonds		127	232	99	48	2.2	17.0	0.8	
D,L-*N*-acetyl-L-amide	(D,L-NALA)	116	233	93	23	7.8	12.2	−2.4	29
with H bonds		126	244	84	49	11.5	13.8	−1.1	
L−*N*-acetyl-G-amide	(NAGA)	95	193	80	10	11.8	14.0	4.6	29
with H bonds		111	213	79	32	6.1	17.7	4.8	
N-acetyl-E	(NAE)	102	218	82	5	2.3	12.7	0.5	23
with H bonds		114	232	73	36	2.8	12.4	0.4	
N-acetyl-P*G -amide	(NAPGA)	103	213	63	34	0.1	18.8	0.1	31
with H bonds		94	193	64	24	2.1	18.8	−4.8	
N-acetyl-V-amide	(NAVA)	117	226	98	27	2.5	12.1	−1.2	30
with H bonds		130	246	88	54	4.3	14.4	−1.6	
N-acetyl-G	(NAG)	90	198	88	−18	13.3	20.0	0.9	24
with H bonds		100	215	81	4	13.1	19.7	3.4	
experimental		113	220	83	37	25 ± 5	25.5 ± 1	−	4
GG·HCl·H_{2O}	(GG·HCl	109	199	88	39	26.6	15.9	4.6	26
with H bonds	·H_2O)	120	216	74	68	24.4	20.3	5.4	
experimental		116	216	71	60	−	21.3	1.0	7
		111	210	64	59	−	25 ± 5	−	44
N-acetyl-*VL-amide	(NAVL)	122	222	111	32	47.5	6.1	4.6	23
with H bonds		129	236	99	52	34.0	7.6	4.1	
experimental		126	230	87	60	34 ± 12	20 ± 2	−	45
N-acetyl-V*L-amide	(NAVL)	117	226	98	26	15.2	14.6	−4.6	23
with H bonds		127	243	86	52	16.6	16.2	−4.2	
experimental		128	232	93	58	36 ± 11	18 ± 2	−	45
N-acetyl-V	(NAV)	112	215	94	25	6.7	16.5	−5.0	23
with H bonds		127	240	89	53	2.2	16.6	−3.7	
experimental		121	225	81	56	20 ± 15	21 ± 2	−	45

[a] The principal elements of CSA tensor (σ_{iiN}, $ii = 11, 22, 33$) and the isotropic chemical shift (σ_{isoN}) are given in ppm relative to liquid ammonia at 25 °C (the absolute shielding 244.6 ppm is set to zero ppm). [b] α_N, β_N, and γ_N are given in degrees.

2. Only the symmetric tensor is secular with respect to the Zeeman interaction and consequently is the only part evident in standard solid-state NMR experiments. For this reason, only the symmetric part of the calculated CSA tensors is reported in this paper. It should be noted here that the antisymmetric part of the CSA tensor can have an effect on spin relaxation rates in certain experiments.[2,14] Experimentally, a CSA tensor is measured relative to a given reference. An absolute shielding of 244.6 ppm for liquid ammonia at 25 °C was therefore used to convert calculated shieldings to the IUPAC chemical shift scale.[41]

The accurate calculation of chemical shifts with precision requires the positions of all atoms to be known with precision. X-ray crystallography cannot provide accurate positions for atoms that do not scatter X-rays efficiently. Therefore, the positions of hydrogen atoms are not known with certainty even in highly resolved crystal structures such as the ones used here. The errors in the bond lengths and angles of hydrogen atoms due to this uncertainty can have a dramatic effect on the calculated CSA tensor. For example, a factor-of-two improvement in the orientation of ^{13}C CSA tensors in terpenes was noted after a partial ab initio optimization of the position of hydrogen atoms in the crystal structure.[42] A similar improvement in the ^{15}N chemical shifts of chlorophylls was noticed after optimization of the original crystal structures.[43] To see if a similar improvement could be made for amide ^{15}N CSA tensors a second set of calculations was performed after the positions of the hydrogen atoms in the crystal structure were optimized with the heavy atoms fixed in position. Density functional theory with a 6-31G* basis set and Becke's three-parameter hybrid correlation functional was used.[44] This level of calculation has been previously shown to give hydrogen atom positions comparable to neutron-diffraction values for a wide variety of systems.[42,43,45] The neutron diffraction structures of *N*-acetyl cysteine (NAC) and GG·HCl·H_2O, in which the positions of the hydrogen atoms are known to a high accuracy, were not optimized.[34,26]

Results and Discussion

Orientation of the ^{15}N CSA Tensor. β_N Angle. The ab initio amide site ^{15}N CSA tensors obtained from the nonoptimized structures and optimized structures are summarized with the available experimental values in Tables 1 and 2, respectively.

(41) Jameson, C. J.; Jameson, A. K.; Cohen, S. M.; Parker, H.; Opposunggu, D.; Burrell, P. M.; Wille, W. *J. Chem. Phys*. **1981**, *74*, 1608.

(42) Harper, J. K.; McGeorge, G.; Grant, D. M. *Magn. Reson. Chem.* **1998**, *36*, S135−S144. Harper, J. K.; McGeorge, G.; Grant, D. M. *J. Am. Chem. Soc.* **1999**, *121*, 6488−6496.

(43) Facelli, J. C. *J. Phys. Chem. B* **1998**, *102*, 2111−2116.

(44) Becke, A. D. *J. Chem. Phys.* **1993**, *98*, 5648−5652.

(45) Facelli, J. C.; Pugmire, R. J.; Grant, D. M. *J. Am. Chem. Soc.* **1996**, *118*, 5488−5489.

Table 2. Quantum Chemical Calculations of Amide-^{15}N Chemical Shift Tensors in Peptides from Optimized Structures

molecule		σ_{isoN}	σ_{33N}[a]	σ_{22N}	σ_{11N}	α_N[b]	β_N	γ_N	ref
D,L-*N*-acetyl-A-amide	(D,L-NAA)	126	226	115	39	10.0	15.4	−13.2	27
with H bonds		135	244	96	64	4.4	17.7	−15.7	
L- *N*-acetyl-A-amide	(L-NAA)	130	229	115	47	20.2	14.8	−8.7	29
with H bonds		140	245	101	74	5.8	17.5	11.9	
N-acetyl-*AA-amide	(NAAAA)	129	228	109	50	5.0	17.0	1.0	32
with H bonds		139	246	98	74	5.8	17.4	−0.7	
N-acetyl-A*A-amide	(NAAAA)	120	209	104	46	3.8	17.0	8.4	32
with H bonds		132	231	92	75	9.6	18.1	−9.9	
N-acetyl-G*A-amide	(NAGAA)	127	226	126	30	16.6	15.4	−4.1	32
with H bonds		136	248	100	61	19.1	17.2	−5.3	
N-acetyl-*GA-amide	(NAGAA)	111	207	97	30	17.4	16.8	3.2	32
with H bonds		122	226	87	53	13.1	19.4	−8.0	
experimental		120	229	85	45	−	20.7 ± 2	−	42
N-acetyl-M	(NAM)	128	221	126	36	34.2	18.0	−11.7	28
with H bonds		130	228	109	53	27.0	17.8	−9.7	
N-acetyl-C	(NAC)	115	214	107	24	3.0	17.6	0.1	34
with H bonds		127	232	99	48	2.2	17.0	0.8	
D,L-*N*-acetyl-L-amide	(D,L-NALA)	142	228	135	62	9.4	16.1	11.5	29
with H bonds		151	247	115	93	6.7	17.9	−13.0	
L-*N*-acetyl-G-amide	(NAGA)	111	206	97	30	27.9	14.2	8.5	29
with H bonds		118	218	89	49	17.3	18.7	−8.5	
N-acetyl-E	(NAE)	115	203	100	43	22.0	20.0	−8.5	23
with H bond		121	213	85	65	21.0	20.9	−8.4	
N-acetyl-P*G -amide	(NAPGA)	104	196	83	34	41.8	22.4	−16.4	31
with H bonds		119	219	77	59	29.3	24.0	−16.1	
N-acetyl-V-amide	(NAVA)	121	212	108	42	38.1	19.8	−9.8	30
with H bonds		135	236	98	70	27.8	20.7	−11.9	
N-acetyl-G	(NAG)	111	202	113	18	4.1	23.7	3.2	24
with H bonds		112	216	92	28	0.7	22.5	−0.5	
experimental		113	220	83	37	25 ± 5	25.5 ± 1	−	4
GG·HCl·H_2O	(GG·HCl	109	199	88	39	26.6	15.9	4.6	26
with H bonds	·H_2O)	120	216	74	68	24.4	20.3	5.4	
experimental		116	216	71	60	−	21.3	1.0	7
		111	210	64	59	−	25 ± 5	−	44
N-acetyl-*VL-amide	(NAVL)	129	219	116	52	26.8	15.8	4.6	23
with H bonds		133	227	100	72	6.1	18.4	7.9	
experimental		126	230	87	60	34 ± 12	20 ± 2	−	45
N-acetyl-V*L-amide	(NAVL)	133	230	129	40	5.6	14.8	−4.6	23
with H bonds		144	253	107	73	1.8	17.8	2.0	
experimental		128	232	93	58	36 ± 11	18 ± 2	−	45
N-acetyl-V	(NAV)	119	214	105	39	21.4	21.0	−13.4	23
with H bonds		133	234	98	66	11.6	20.7	−12.1	
experimental		121	225	81	56	20 ± 15	21 ± 2	−	45

[a] The principal elements of CSA tensor (σ_{iiN}, $ii = 11, 22, 33$) and the isotropic chemical shift (σ_{isoN}) are given in ppm relative to liquid ammonia at 25 °C (the absolute shielding 244.6 ppm is set to zero ppm). [b] α_N, β_N, and γ_N are given in degrees.

The overall distribution of ab initio β_N Euler angles, calculated using the original crystallographic coordinates, qualitatively resembles the experimental distribution of β_N but has several features which are noticeably different. Experimentally, the amide site β_N angles determined from solid-state NMR experiments range from around 16.5° to 25.5° with most within ±2° of 18°. By comparison, the distribution of ab initio β_N values is wider (6°−22°) for the nonoptimized structures and the median value is around 15° instead of 18°. On the other hand, the ab initio β_N Euler angle distribution for the optimized structures more closely resembles the experimental solid-state NMR distribution with the bulk of the β_N values clustered in a narrow range around 17.5°−18.5°. The majority of the remainder of the β_N values are between 18.5° and 22.5°, with only two β_N angles less than 17°. The range of β_N for optimized structures reported here is also in agreement with a previous ab initio study on glycyl−glycine conformers where a β_N range of 18.4−22.4° was found using a SOS (sum-over-states) density functional approach.[8]

An alternative definition of β_N is used when the CSA tensor is characterized using the dipolar axis of the N−C_1 bond instead of the N−H bond. In this definition β_N is the angle between the σ_{33N} axis and the C_1−N bond. The range of the ab initio values using this alternative definition is from 95° to 105° for both sets of structures, also within the reported solid-state NMR experimental range.

The β_N values for six of the ^{15}N CSA tensors studied in this work are available experimentally and their results are considered in greater detail below.

The wealth of experimental data available about the GG·HCl·H_2O molecule makes the molecule an excellent test of the accuracy of the ab initio method. The coordinates are known with high precision from neutron scattering experiments eliminating the possibility of an erroneous experimental geometry as a source of error in the calculation.[26] In addition, the ^{15}N CSA tensor orientation has been determined independently from both a dipolar−chemical shift correlation and from a single-crystal solid-state NMR experiment. The ab initio result of 20.7° is in excellent agreement with both the 21° β_N value determined by a single crystal study[7] and the 20 ± 5° value determined by dipolar−chemical shift correlation on a powdered sample.[46]

For the calculations using the crystal structure geometry, only one of the remaining five ab initio β_N angles is within

(46) Munowitz, M.; Aue, W. P.; Griffin, R. G. *J. Chem. Phys.* **1982**, *77*, 1686−1689.

experimental errors of the β_N angle values determined from solid-state NMR studies. Substituting the ab initio calculated β_N value of 16.2° for the experimental β_N angle of 18° changes the simulated spectrum of the leucine residue in NAVL by only about 5% rmsd.[47]

The calculated β_N angle values of the other four ^{15}N CSA tensors calculated using the crystal structure geometry fall outside the experimental error range. In particular, the ab initio calculated β_N angle for the valine residue of the NAVL molecule is significantly different from the experimental value: 7.6° compared to 20°.[47] The unusual N−H−C_1 angle of 103.5° in the crystal structure of the valine residue in NAVL compared to the usual value of 114°−123° is probably the reason for this discrepancy.[23] On the basis of the most recent experimental results, the difference between the β_N angle of 16.6° calculated using the original crystal structure geometry and the experimental β_N angle of 21° would lead to a difference of 10−15% rmsd in the simulated spectrum of NAV.[47] The ab initio value for the β_N angle of NAG, 19.7°, obtained using the crystal structure geometry shows a substantial deviation from the experimental value of 25.5° as well.[4] The experimental β_N value for NAGAA was reported to be 100.0° using the alternative definition of β_N as the angle between the σ_{33N} axis and the C_1−N bond.[48] This β_N value corresponds to 20.5° in our definition which was obtained using the crystal structure C_1−N−H bond angle of 120.5°. The ab initio β_N angle therefore shows a 2.5° deviation from the experimental value.

The ab initio β_N values based on the optimized structures fare much better than ab initio β_N values based on the nonoptimized structures in comparison to experimental data. Four out of five ab initio β_N values of the optimized structures are within experimental errors of their experimental value. Most significantly, the β_N angle for the valine residue in the new optimized structure of the NAVL molecule is calculated to be 18.4° which is much closer to the experimental value of 20° based on the latest experimental determination.[47] In fact, the ab initio β_N value only changes the simulated spectrum of NAVL by 5−10% rmsd when substituted for the experimental β_N value. The geometry around the leucine residue in NAVL did not change as dramatically during optimization but the new ab initio value of 17.8° is still a significant improvement over the crystal structure β_N value of 16.2° when compared to the experimental β_N angle of 18 ± 2°.

Optimization of the hydrogen atom positions in NAV, NAG, and NAGAA also improved the agreement of the ab initio β_N angles with experimental results. The new ab initio β_N angle of 20.7° in the optimized structure of NAV is in excellent agreement with the experimental 21° angle. Using the C1−N−H angle of 120.7° in the optimized structure of NAGAA, the ab initio β_N value of 19.4° can be seen to be in agreement with the experimental value (100.0°).[48] The only β_N value that falls outside the experimental errors is that of NAG for which the ab initio β_N value of 22.5° is in closer, but not in complete, agreement with the experimental value.

α_N Angle. The distribution statistics for the ab initio α_N angles from optimized structures and nonoptimized structures are similar with the α_N values being more or less evenly distributed in the range from 0° and 35° in both cases. Most ^{15}N solid-state NMR studies on peptides have reported α_N to be 0° within a relatively large uncertainty.[9,48−50] However the ab initio α_N angles in this study are less than 5° for less than six of the eighteen CSA tensors with the remainder being mostly in the 10−20° range. This discrepancy in the value of α_N can be partly attributed to the large uncertainty inherent in the solid-state NMR experimental measurement of α_N. In most peptides the ^{15}N CSA tensor is nearly axially symmetric with the magnitude of σ_{11N} being only slightly less than the magnitude of σ_{22N}. The near degeneracy in the calculated magnitudes of σ_{11N} and σ_{22N} principal elements obscures changes in their relative positions, and as a result experimental determination of α_N angle is difficult and imprecise. In the absence of compelling evidence to the contrary, most studies in the literature have assumed the angle α_N to be 0° strictly based on symmetry arguments. The symmetry argument is based on an idealized description of an amide site. The peptide plane is imagined to be strictly planar and approximating the environment around the ^{15}N nucleus by considering only the immediate symmetry around the amide site. The idealized model predicts one of the ^{15}N CSA components will be perpendicular to the peptide plane and the other two components will lie within the peptide plane yielding 0° for both α_N and γ_N angles. In reality neither of these conditions holds true in real peptides. First, the X-ray crystal structures of the peptides in this study show a 2−5° deviation from perfect planarity of the peptide plane. This prediction is in good agreement with NMR studies reported in the literature where a change up to ∼5° in the planarity of the peptide bond is predicted on the basis of the scalar couplings measured using solution NMR experiments.[51] More importantly, the ^{15}N CSA tensor is known to be affected by more than the immediate bonds around the amide site. This can be seen in the well-known correlation between secondary structure and the components of the ^{15}N CSA tensor in both experimental and theoretical chemical shift measurements.[5,52] Quantitatively, the anisotropy of the CSA tensor of a given nucleus can be expressed as a function of the isotropic average of the shielding in the surrounding space using the following relation:

$$\sigma_{ij}(\mathbf{R}) - \sigma_{iso}(\mathbf{R})\delta_{ij} = \int\left\{\frac{(\mathbf{r}-\mathbf{R})_i - (\mathbf{r}-\mathbf{R})_j}{|\mathbf{r}-\mathbf{R}|^5} - \frac{\delta_{ij}}{3|\mathbf{r}-\mathbf{R}|^5}\right\}\frac{9\sigma_{iso}(\mathbf{r})}{8\pi}d\mathbf{r}$$

where **R** is a vector describing the coordinates of the nucleus.[12] From this equation it can be shown that the symmetry of the ^{15}N CSA tensor is destroyed by the effect of nearby atoms that are not in the peptide plane. The consequence of nonplanar peptide planes and the out-of-plane polarization of the electron density around the ^{15}N nucleus due to nonbonded interactions is that the α_N and γ_N angles in peptide ^{15}N CSA tensors are no longer required to be zero by symmetry. In fact, careful reexamination of α_N in systems where previously it was thought to be zero has led to its experimental reevaluation to a nonzero value in some cases.[4,9,47] For example, the α_N angle value for the Gly2 residue of Gramicidin A has been reevaluated from 0° to 28°,[9,49] the α_N angle in NAV molecule has been reevaluated from 0° to 20°,[47,50] and the α_N angle in NAG has been reevaluated from 0° to 25°.[4,50]

(47) Lee, D. K.; Wei, Y.; Ramamoorthy, A. *J. Phys. Chem.* Submitted for the publication.

(48) Oas, T. G.; Hartzell, C. J.; Dahlquist, F. W.; Drobny, G. P. *J. Am. Chem. Soc.* **1987**, *109*, 5962−5966.

(49) Teng, Q.; Cross, T. A. *J. Magn. Reson.* **1989**, *85*, 439−447.

(50) Roberts, J. E.; Harbison, G. S.; Munowitz, M. G.; Herzfeld, J.; Griffin, R. G. *J. Am. Chem. Soc.* **1987**, *109*, 4163−4169. Wang, A. C.; Bax, A. *J. Am. Chem. Soc.* **1996**, *118*, 2483−2494. Hu, J. S.; Bax, A. *J. Am. Chem. Soc.* **1997**, *119*, 6360−6272. Tjandra, N.; Grzesiek, S.; Bax, A. *J. Am. Chem. Soc.* **1996**, *118*, 6264−6272.

(51) Oldfield, E. *J. Biomol. NMR* **1995**, *5*, 217−225.

(52) Lumsden, M. D.; Wu, G.; Wasylishen, R. E.; Curtis, R. D. *J. Am. Chem. Soc.* **1993**, *115*, 2825−2832. Moore, R. A. *Chem. Phys. Lett.* **2000**, *4*, 360−364.

Only four α_N experimental angles are available for the molecule considered in this study. Experimental limitations prevented α_N from being measured for two of the molecules for which β_N angles were available. The near axial symmetry of the ^{15}N CSA tensor in GG·HCl·H_2O prevented the α_N angle from being determined experimentally while the ab initio calculations yielded a value of 22.2° for the α_N angle.[7,46] During the experimental measurement of the ^{15}N CSA tensor orientation of NAGAA α_N was assumed to be 0°.[48] The ab initio values of 4.1° for the nonoptimized structure and 1.5° for the optimized structure are in good agreement with this assumption.

The α_N angles of NAV and NAG were originally assumed to be zero as well.[50] However, the most recent estimate for α_N in NAV is 20°, with the simulated spectrum being insensitive to changes in α_N with angles between 0° and 34° only having a 5% rmsd change in the simulated spectrum compared to experiment.[47] The α_N angle of 5.2° calculated from the original geometry and the α_N angle of 11.6° calculated from the new partially optimized geometry can both be considered to be in relatively good agreement with experimental results because of this insensitivity of the simulated spectrum to variations in α_N.

For the NAG molecule, ab initio calculations using the original geometry yielded an α_N value of 13.7°, in good agreement, within experimental errors, with the experimental value of 25°.[4] The α_N angle of the optimized structure is 0.7°. Since α_N is determined with much less precision experimentally than β_N, the overall agreement of the calculated CSA tensor with experimental results is still better for the optimized crystal structure. This is also the case for NAVL as well, for which the α_N ab initio values of the nonoptimized structures are in closer agreement with the experimental results than the α_N ab initio values of optimized structures.[47]

γ_N Angle. As mentioned above, the Euler angle γ_N is not measured directly through a single correlation of chemical shift and dipolar coupling parameters. Since γ_N is needed to position the ^{15}N CSA tensor in the molecular frame, solid-state NMR spectra obtained from powder samples have always been interpreted by assuming that the least shielded axis of the ^{15}N CSA tensor, σ_{33N}, lies within the peptide plane. This assumption is equivalent to setting $\gamma_N = 0°$. A nonzero γ_N angle could lead to errors in the experimental prediction of the directions of the σ_{11N} and σ_{22N} axes relative to the molecular frame. This does not imply that the experimentally determined α_N values are wrong as most of the solid-state NMR experiments on powder samples provide the orientation of the ^{15}N CSA relative to the N−H bond only. On the other hand, if σ_{33N} in reality is not in the peptide plane, then the interpretation of α_N angles in terms of the orientation of the σ_{11N} (or σ_{22N}) axis relative to the molecular frame might be led astray by the zero γ_N angle approximation.

The only direct experimental evidence for the coincidence of the σ_{33N} axis with the peptide plane comes from the GG·HCl·H_2O single crystal study for which σ_{33N} deviates from the peptide plane by only 1°.[7] A 3.8° γ_N angle is predicted by the calculations for the GG·HCl·H_2O molecule. The ab initio calculations on average predict ~4° deviation of the σ_{33N} axis from the peptide plane as shown by the γ_N angles in Table 1. The lack of experimental data makes an evaluation of the zero γ_N approximation difficult. It is possible that peptides other than GG·HCl·H_2O do have nonzero γ_N angles. However, in the GG·HCl·H_2O molecule, the only case where an experimental γ_N angle value is available, the ab initio calculations predicted γ_N to be 3.8° as compared to the experimental value of 1° determined from the single-crystal study. As can be seen in Tables 1 and 2 most of the ab initio calculated γ_N angles are less than 5°. The only other ab initio γ_N values available are from a study by Walling et al. who found γ_N to be less than 1° for extended and β-sheet conformations of a model dipeptide and 5.5° for the α helix conformation.[8] Without strong experimental evidence to the contrary, it seems reasonable to conclude at this point that γ_N is in reality very close to 0°.

Table 3. Basis Set Dependence of Amide-^{15}N Chemical Shift Tensors in Peptides

		σ_{isoN}	σ_{11N}[a]	σ_{22N}	σ_{33N}	α[b]	β	γ
NAC	STO-3G	17	85	9	−44	5.5	20.0	−2.0
	4-31G	102	198	87	21	7.9	18.7	−1.5
	6-31G	101	197	86	19	8.2	18.6	−1.6
	6-31G(d,p)	100	190	88	21	7.0	17.9	−1.3
	6-311G	120	222	107	31	5.5	17.3	−0.6
	6-311G(2d,p)	115	214	107	24	3.0	17.6	0.1
	6-311+G(2d,p)	120	222	107	31	5.3	17.3	−0.6
	6-311++G(2d,p)	120	222	107	31	5.5	17.3	−0.6
L-NAA	STO-3G	118	225	105	24	8.8	12.7	4.2
	4-31G	109	206	97	24	9.7	13.0	4.4
	6-31G	108	205	96	24	9.8	12.6	4.3
	6-31G(d,p)	105	197	95	24	7.6	12.4	3.9
	6-311G	118	225	105	24	8.8	12.7	4.2
	6-311G(2d,p)	123	226	114	29	10.1	11.8	4.3
	6-311+G(2d,p)	127	232	114	35	7.7	11.7	3.9
	6-311++G(2d,p)	127	232	114	35	7.4	11.7	3.9
NAG	STO-3G	1	78	4	−79	15.1	21.2	6.8
	4-31G	78	183	72	−21	13.0	20.7	5.8
	6-31G	77	183	70	−22	12.9	20.5	5.7
	6-31G(d,p)	75	175	71	−21	12.7	20.3	5.6
	6-311G(d,p)	88	194	90	−20	13.3	20.5	5.9
	6-311G(2d,p)	90	198	89	−17	13.3	20.0	5.8
	6-311+G(2d,p)	94	206	88	−11	13.0	19.6	5.7
	6-311++G(2d,p)	95	207	88	−10	13.0	19.6	5.5

[a] The principal elements of CSA tensor (σ_{iiN}, ii = 11, 22, 33) and the isotropic chemical shift (σ_{isoN}) are given in ppm relative to liquid ammonia at 25 °C (the absolute shielding 244.6 ppm is set to zero ppm). [b] α_N, β_N, and γ_N are given in degrees.

Basis Set Convergence of the ^{15}N CSA Orientation. An important goal for quantum chemical calculations is to reproduce CSA tensor orientations not just for small model peptides but for larger, biologically relevant polypeptides. Unfortunately the locally dense scheme outlined above is impractical for determining ^{15}N CSA tensor orientations at multiple sites along a peptide. These basis sets were selected because they have been previously shown to be near the convergence limit for reproducing the magnitudes of the ^{15}N CSA tensor.[36] Since the orientation of the ^{15}N CSA tensor is primarily determined directly by the geometry of the bonds around the amide site, it should be less sensitive to small changes in bond energetics that strongly affect the principal values of the CSA tensor. It should then be possible to accurately reproduce CSA tensor orientations with much smaller basis sets than those necessary to accurately reproduce chemical shifts. This has previously been shown to be true for ^{15}N CSA tensors in heterocyclic organic compounds.[53] To test this hypothesis on amide nitrogen ^{15}N systems another set of calculations were done on each molecule using the following smaller basis sets: 6-31G, 6-31G(d,p), 4-31G, STO-3G, 6-311G(d,p), and 6-311G. Test calculations with larger basis sets with diffuse functions 6-311+G(2d,p), 6-311+G(3df,2p), and 6-311++G(2d,p) were also performed to check the convergence of the previous calculations with respect to diffuse functions. The results are shown in Table 3.

The ^{15}N CSA tensor orientations show a striking insensitivity to the size of the basis function as compared to the principal values of the CSA tensor. Even the minimal STO-3G basis set

(53) Brender, J.; Ramamoorthy, A. Unpublished results.

does a fair job of reproducing the CSA tensor orientation; it reproduces the β_N angle calculated at the 6-311G(2d,p) level within 2° and the α_N angle within 4°. Split valence and diffuse functions in particular are essential for accurately reproducing the principal values while they have little effect on the orientation of the CSA tensor. The principal values of the CSA tensor are somewhat less sensitive to the presence of polarization functions but the average 2 ppm deshielding on the addition of polarization functions still comprises a fair amount of the shift range. The largest difference in β_N is around 2°, approximately the experimental uncertainty for the β_N angle in most powder samples measured using solid-state NMR methods. The largest difference in α_N is of the order of the experimental error of 5°. Furthermore, the use of larger basis sets does not appear to systematically improve the CSA tensor orientation. Smaller basis sets appear to be sufficient to determine the CSA orientation in the molecular frame. This property makes possible the study of CSA tensor orientations in large (150 or more atoms) biomolecules.

Chemical Shifts. The isotropic chemical shift and the magnitudes of the three principal elements of the ^{15}N CSA tensor are listed in Table 1. In contrast to the orientation of the ^{15}N CSA tensor the principal values have been the subject of numerous theoretical and experimental studies. These studies have been primarily aimed at deducing the relationship between the isotropic chemical shift and geometrical parameters such as dihedral angles. Such studies have shown that even though the calculated chemical shifts of model peptides mimic the experimentally predicted correlation between secondary structure and chemical shift, the absolute value of the chemical shift calculated from real peptides often show a significant discrepancy from the experimentally observed values similar to those found here. For example, Le and Oldfield studied the isotropic ^{15}N chemical shifts of 38 alanine residues in DHFR, SNase, and cytochrome *c*550 using Hartree−Fock calculations.[17] A strong correlation between the calculated and experimental ^{15}N isotropic chemical shifts was obtained for cytochrome *c*550. However, the calculated chemical shifts of the alanine residues in DHFR and SNase showed significant deviations from experimental values—as much as 18 ppm for one residue. Since the experimentally reported ^{15}N chemical shift range in proteins is only 20 ppm, this is not likely to be reliable for applications where a quantitative measurement is required. The individual CSA tensor components show an even larger discrepancy; this is mainly due to the cancellation of errors in the calculation of σ_{11N} and σ_{33N} components as can be seen from Table 1 and Table 2.

The error in the absolute values of chemical shifts obtained from the calculations can be attributed to both errors in the experimental geometries used and to deficiencies in the method used to calculate the chemical shift. As mentioned above, the largest source of error comes from the poor resolution of hydrogen atoms in the X-ray crystal structures used as geometries for the structures in the chemical shift calculations. This is a much more severe problem for the quantitative prediction of chemical shifts than for the determination of CSA tensor orientations. This is because while α_N and β_N are insensitive to changes in bond length the derivative of the shielding with respect to changes in bond lengths can be as high as 300 ppm per Å.[13]

Even when a high precision neutron diffraction structure is available, as is the case for GG·HCl·H_2O, the principal components of the CSA tensor are still in error by about ∼5 ppm. Therefore, the remainder of the error can be assumed to come from deficiencies in the ab initio method that is used to calculate the shielding tensors. Assuming a correct starting geometry, there are three sources of errors that may cause the ab initio method to falter and to predict incorrect chemical shifts. The first is an insufficient basis set. In particular the diffuse functions left out for reasons of computational efficiency in the calculations of ^{15}N CSA tensor orientation were shown to be important for quantitative prediction of ^{15}N chemical shifts as shown in Table 3. These results predict that the diffuse functions will increase the shielding of σ_{11N} and σ_{33N} over that listed in Table 1 by approximately 5−7 ppm while lowering the shielding of σ_{22N} by around 2−5 ppm. The second source of error is improper inclusion of intermolecular interactions. Since the full hydrogen-bonding network was included for all NAGAA, only the effect of long-range electrostatic interactions must be considered. Some studies have found that the ^{15}N CSA tensor is affected by as much as 20 ppm with the inclusion of point charges.[2] Other studies have found a more moderate change of about 10 ppm upon incorporation of long-range intermolecular effects.[5,15] It can be expected that zwitterionic and charged molecules such as GG·HCl·H_2O will be more strongly influenced by long-range electrostatic effects. The final possible defect is the improper incorporation of electron correlation effects. Although a detailed study is missing, an incorrect isotropic radial dependence of the electron density presumably would have a much smaller effect on the orientation of the ^{15}N CSA tensor than on the magnitude of the principal elements of the CSA tensor.

The Effect of Hydrogen Bonding. The influence of hydrogen bonding on CSA is of considerable interest both for the interpretation of experimental data and for the efficient implementation of computational methods. As can be seen from Tables 1 and 2, hydrogen bonding was found to have little influence on the orientation of the amide ^{15}N CSA tensor relative to the molecular frame in most cases. This is in agreement with the previous ab initio studies on ^{15}N CSA tensors in model dipeptides.[8,18] The ^{15}N CSA tensor stands in contrast to the $^{13}C_1$ CSA tensor and the amide ^{1}H CSA tensor where large changes in orientation were discovered in response to both hydrogen bonding and to long-range electrostatic effects.[8,16] In the nonoptimized structures, the largest change in β_N upon hydrogen bonding is 4.3° with the average change being only 1.3°. The largest change in β_N upon hydrogen bonding in the optimized structures is 4.5° with an average change of 1.9°. Nine out of eighteen ^{15}N CSA tensors of the nonoptimized structures, and six out of eighteen of the optimized structures, show a change of less than 1° in the value of β_N angle on hydrogen bonding. The general effect of hydrogen bonding appears to bend σ_{33} away from the N−H bond. Hydrogen bonding has a larger effect on α_N than β_N values. In the nonoptimized structures the average change in α_N is 2.6°, and the largest change is 9.9°, whereas in the optimized structures the average change in α_N is 6.7°, and the largest change is 20.2°. The insensitivity of the ^{15}N CSA tensor orientation to hydrogen bonding is striking in contrast to the marked effect it has on the magnitudes of the principal elements of the ^{15}N CSA tensor as can be seen from Tables 1 and 2. Hydrogen bonding was found to deshield the isotropic chemical shift by as much as 10 ppm in both cases. The change in anisotropy is even greater with σ_{11N} changing by about 25 ppm on average.

Conclusions

The results published here show that the ab initio calculations show promise in the quantitative prediction of ^{15}N CSA tensor

orientations. The results from this study suggest that the orientation as well as the magnitudes of ^{15}N CSA tensors may vary from molecule to molecule. In addition, the ^{15}N CSA tensor was found to be quite sensitive to the geometry used in the calculation. Initial results based directly on X-ray geometries showed promising agreement in some cases but faulty values in others. Five of the six tensors for which experimental β_N Euler angles were known were calculated within experimental errors after optimization of the positions of hydrogen atoms in the crystal structure geometry. This suggests that there is a possibility of using CSA tensors in optimizing positions of H atoms in X-ray determined structures. The accuracy of the other Euler angles, α_N and γ_N, is more difficult to estimate because of the lack of reliable experimental data and their complex dependence on geometrical parameters. Nevertheless, the nonzero variation in the value of α_N angle predicted from our studies is in relatively good agreement with recent solid-state NMR experimental studies. Also, a γ_N angle averaging $0-5°$ predicted by our studies is in close agreement with the only available experimental result and other ab initio studies.

An important question in computational chemistry is the level of calculation and the size of the system that must be required to accurately reproduce experimental values. In agreement with previous studies, the ^{15}N CSA tensor orientation was shown in most cases not to depend significantly on hydrogen bonding. Our results also show that the orientation of the tensor can also be calculated accurately with much smaller basis sets than are needed for accurate computation of the magnitudes of the principal elements of the CSA tensor. Therefore, the size of the system for which orientations of ^{15}N CSA tensors can be calculated quantitatively is much larger than the size of the system for which the chemical shifts can be calculated quantitatively. We hope that the ready availability of ^{15}N CSA tensor orientations through ab initio studies will have a significant impact on the structural studies of proteins using NMR spectroscopy. In addition, the data reported here should be valuable in the development of solid-state NMR techniques to measure ^{15}N CSA tensors from powder samples.

Acknowledgment. This research was partly supported by NSF through Grant MCB-9875756 (CAREER Development Award to A.R.).

JA001980Q